

1 Fractionation of Squid Pens with Ionic Liquids – An upgraded β -Chitin 2 and Shellfish Protein Production

3 Nakasu, P.Y.S.¹; Piccoli, V.³; Ovejero-Pérez, A.¹; Kumar, P¹; Al Ghatta, A. ¹; Melanie, S²; Polesca,
4 C⁴; Martínez, L. ³; Hallett, J.P.¹

5 1. Department of Chemical Engineering, Imperial College London, SW7 2AZ, London- UK

6 2. Department of Materials, Imperial College London, SW7 2AZ, London- UK

7 3. Department of Physical Chemistry, Institute of Chemistry, Universidade Estadual de
8 Campinas (UNICAMP), CEP 13083-862, Campinas-BR.

9 4. CICECO – Aveiro Institute of Materials, Department of Chemistry, University of Aveiro,
10 3810-193 Aveiro, Portugal

11 5. The National Research and Innovation Agency of the Republic of Indonesia (BRIN), Jakarta,
12 Indonesia

13

14 **Abstract:**

15 In this work, the foundation of a biobased ionic liquid utilization of squid waste has been scrutinized.

16 An ionic liquid screening showed that the biocompatible ionic liquid choline acetate, [Ch][OAc], can

17 extract more than 80 wt% of the protein and precipitate it upon solvent swing between ethanol and

18 water. Process parameter optimization was carried out with factorial design of experiments to yield 75%

19 of recovered protein with an estimated 90% purity and a highly acetylated, crystalline β -chitin with up

20 to 95% purity. Physico-chemical analyses of these two streams confirmed the efficiency of ionic liquid

21 separation and the amino acid profiling of the protein isolate revealed the presence of three major

22 essential amino acids, histidine, leucine and valine that could be a valuable alternative protein source

23 for feed in aquaculture. Molecular dynamic simulations show that the affinity of [OAc]⁻ to protein

24 surfaces is greater than that of alternative anions, facilitating protein solubilization. However, its

25 combination with [Ch]⁺ is optimal because the interactions of this cation with the protein surface are

26 relatively weak, allowing the protein to be recovered from the IL. A material mass balance of the process

27 has shown the solvent usage is high, which ultimately impacts on high energetic requirements. Techno-

28 economic confirmed that solvent usage makes up to nearly 65% of the minimum selling price of the

29 protein, which reaches up to 9 \$/kg, but decreases with co-production of β -chitin down to 0.6 \$·kg⁻¹ for

30 each 1 \$·kg⁻¹ of chitin. Solvent usage also impacts negatively on CO₂ emissions with up to 4.27 kg

31 CO₂·kg⁻¹ of product. These emissions are split into 61% for the protein and 39% for the β -chitin

32 production.

33 **Keywords:** Process design, Squid waste, techno-economic analysis, molecular dynamics, alternative
34 protein.

35 Seafood is a highly traded global food commodity, and it encompasses a wide range of species,
36 including freshwater and marine finfish, bivalves, decapods, cephalopods, algae, and cyanobacteria¹. In
37 2020, global seafood production reached 214 million tonnes, with the squid fishery representing about
38 4.3 percent of all marine catches by volume and about 7% by value worldwide^{1,2}. The Food and
39 Agricultural Organization of the United Nations estimates the seafood trade to be worth USD 151
40 billion, with a projected 13% growth in production value by 2030. Seafood categories are generally
41 considered to have better environmental performance compared to other protein-rich foods, particularly
42 in terms of sustainability³. However, the seafood supply faces various challenges, including increasing
43 demand due to overfishing, species depletion, environmental pollution, global warming, and
44 biodiversity changes that ultimately have impacted the squid population over the last decades⁴.

45 Interest in the bio-refining of seafood waste through environmentally friendly processing is a result of
46 a growing understanding of how traditional fishing processes affect the environment and the stringent
47 pollution control requirements imposed by regulatory bodies^{3,5}. Squids differ from fish by their high
48 growth rate, short life span, and high feeding behaviour. These characteristics end up exerting a high
49 predation pressure on zooplankton, fish, and other squid prey, as in the case of the invasive Humboldt
50 squid in the eastern North Pacific^{4,6}. There is then a necessity for population control and, of course, the
51 introduction of biorefinery strategies for completely sustainable consumption and utilization of squid
52 waste.

53 Large amounts of squid waste are produced from wild-caught fisheries. It is estimated that more than
54 40% of the total body weight of squid ends up as processing byproducts, including the viscera, pens,
55 and skins⁷. These byproducts are routinely dumped in landfills or released into bodies of water.
56 Incineration, composting, and anaerobic digestion could be an alternative, but only in more developed
57 countries such as the UK and Australia, with disposal costs up to 150 US\$ per tonne⁸. This introduces
58 demand for the implementation of efficient and cutting-edge treatment and utilization methods to

59 minimize any adverse environmental effects on aquatic ecosystems or land and to encourage more
60 productive practices that minimize biomass, energy, or nutrient losses¹.

61 The squid pen, or gladius, is an internalized shell that acts as both a point of attachment for significant
62 muscle groups and a barrier to protect the visceral organs⁹. The pen's distinctive protein and β -chitin
63 composition is what gives it its strength and flexibility. The weight distribution of the pens from
64 different species of squid is 25–49% β -chitin, 43–75% protein, and relatively low ash content⁹. A
65 protein layer surrounds the β -chitin nanofibrils, which are arranged parallel to the pen's long axis by α -
66 helical protein coils^{9,10}.

67 Squid pens valorization has been focused on obtaining protein hydrolysates with antioxidant properties
68 or as fermentation media for microorganisms^{7,11}. These methods, however, do not entail the isolation
69 of the squid protein to obtain a high-purity protein isolate, as the protein recovery methods such as
70 dialysis or membrane separation, would be costly¹². Squid pen utilization for β -chitosan production
71 usually employs harsh chemicals such as hydrochloric acid and sodium hydroxide^{13–15} and generate
72 high volumes of wastewater, which negatively impacts the water footprint of the process¹⁶.

73 Ionic liquids (ILs) are liquid salts at room temperature that present interesting physicochemical
74 properties such as high vapor pressure, conductivity, and high thermal stability. They can be tailored
75 for different purposes by choosing different cation and anion combinations¹⁷. There has been a debate
76 on the 'green-ness' of ILs due principally to their eco-toxicity¹⁸, but this depends on the IL and process
77 configuration. If the IL is fully recovered and the processing water streams are also recycled, then, a
78 greener process can be ensured. Past literature studies entailed solubilizing chitin and chitosan with ILs
79 for energy, pharmaceutical, and medical applications but not the fractionation of shellfish waste. A
80 study by Shamshina and Abidi (2022)¹⁹ has shown that acidic ionic liquids such as 1-butyl-3-
81 methylimidazolium hydrogen sulfate, [BMIM][HSO₄], can efficiently fractionate shrimp shells to
82 produce high-purity chitin. However, there are no studies on holistic biorefinery utilization of squid
83 waste with ILs.

84 In this study, we aim to explore the use of ILs in the fractionation of squid pens to produce high-purity
85 β -chitin and protein as two solid streams. We investigated the influence of the structure of the anion
86 and cation of the IL on protein extraction in an IL screening. Once the IL was chosen, optimization of
87 the fractionation parameters determined the best conditions to ensure high protein yield. Then, recycling
88 of the IL under a limited number of batches was probed to ensure the IL performance was retained along
89 the cycles. Characterization of the produced β -chitin and protein confirmed the efficiency of
90 fractionation. A mass balance of the fractionation process, together with a techno-economic analysis,
91 indicated the process's feasibility. Lastly, molecular dynamic simulation helped us to theorize the
92 explanation of the choline acetate selectivity towards protein extraction and further isolation.

93 **2. Materials and methods**

94 **2.1 Feedstock and reagents**

95 All experiments used European-caught (*Loligo sp.*) squid pens sourced from a fish market in Spain and
96 stored at -80°C . Before fractionation, the squid pens were defrosted, washed in deionized (DI) water,
97 rinsed with ethanol, and dried at 40°C overnight. Then, they were blended into a powder and sieved to
98 a particle size between 180 and 850 μm . Chemicals were sourced from Sigma-Aldrich, UK and
99 included: monoethanolamine (MEA, $\geq 98\%$), methane sulfonic acid (MeSO_3H , $\geq 99\%$), glacial acetic
100 acid (HOAc, 100%), choline bicarbonate ($[\text{Ch}][\text{HCO}_3]$, 80 wt%) and sulphuric acid (H_2SO_4 , 66.3 wt%).

101 **2.2 Squid pen chemical characterization**

102 Squid pens were characterized in a similar procedure by Chaussard and Domard (2004)²⁰. Briefly, the
103 extractive content of squid pens was determined by consecutive 12 h Soxhlet extraction with ethanol
104 and cyclohexane. Then, the squid pens were extracted with $1 \text{ mol}\cdot\text{L}^{-1}$ at 80°C for 3 h for quantitative
105 protein removal; the dry β -chitin mass was considered protein-free after CHN analysis established its
106 nitrogen content was 6.90%. The ash content of the squid pen samples was determined after ashing the
107 dry squid pens in a muffle oven for 6 h at 600°C .

108 **2.2 IL synthesis and characterization**

109 Six ILs were synthesized by dropwise addition of equimolar amounts of the acids – acetic, methane
110 sulfonic, or sulfuric – to the base – choline bicarbonate or monoethanolamine under stirring and cooling
111 with an ice bath (0°C). The six ILs were: choline hydrogen sulfate, [Ch][HSO₄], choline methane
112 sulfonate, [Ch][MeSO₃], choline acetate, [Ch][OAc], monoethanolammonium hydrogen sulfate,
113 [MEA][HSO₄], monoethanolammonium methane sulfonate, [MEA][MeSO₃] and
114 monoethanolammonium acetate, [MEA][OAc]. Once the addition finished, the synthesized IL was
115 allowed to stir for 1 h and had its acid-base ratio and water content adjusted to 1:1 and 20 wt%,
116 respectively. IL water content was measured using a V20 Volumetric Karl-Fischer Titrator (Mettler-
117 Toledo). Acid-base ratios of [Ch][HSO₄] and [MEA][HSO₄] were determined by titration with 0.1M
118 NaOH, using a G20S Compact Titrator (Mettler-Toledo, Columbus, USA), using potassium hydrogen
119 phthalate (Sigma Aldrich, UK) as a primary standard.

120 **2.3 IL screening assays**

121 Briefly, 9.0 g of the IL was added to 1.0 g of squid pen powder in a flat-bottomed glass vial. The vials
122 were then heated to the target temperature in a hot plate with constant stirring at 300 RPM for 3 h in a
123 similar procedure to Polesca et al. (2023)²¹. The vials were then allowed to cool to room temperature,
124 and then 25 mL of ethanol was added. The slurry was filtered, and the filtered solid β-chitin was washed
125 three times with 5 mL ethanol portions. The filtrate had its ethanol content evaporated in a rotary
126 evaporator. Approximately 10 g of DI water was added to precipitate the protein from the IL, the
127 mixture was left sitting for 30 min, and it was centrifuged at 13.3 × G for 10 minutes. The protein was
128 washed thrice with 10 mL DI water and freeze-dried (FreeZone 6, Labconco, MO, USA) to yield a
129 white powder (ESI). β-chitin and protein purity were estimated by CHN analysis (Medac Ltd., UK), the
130 calculations were detailed in the Calculations section 3.

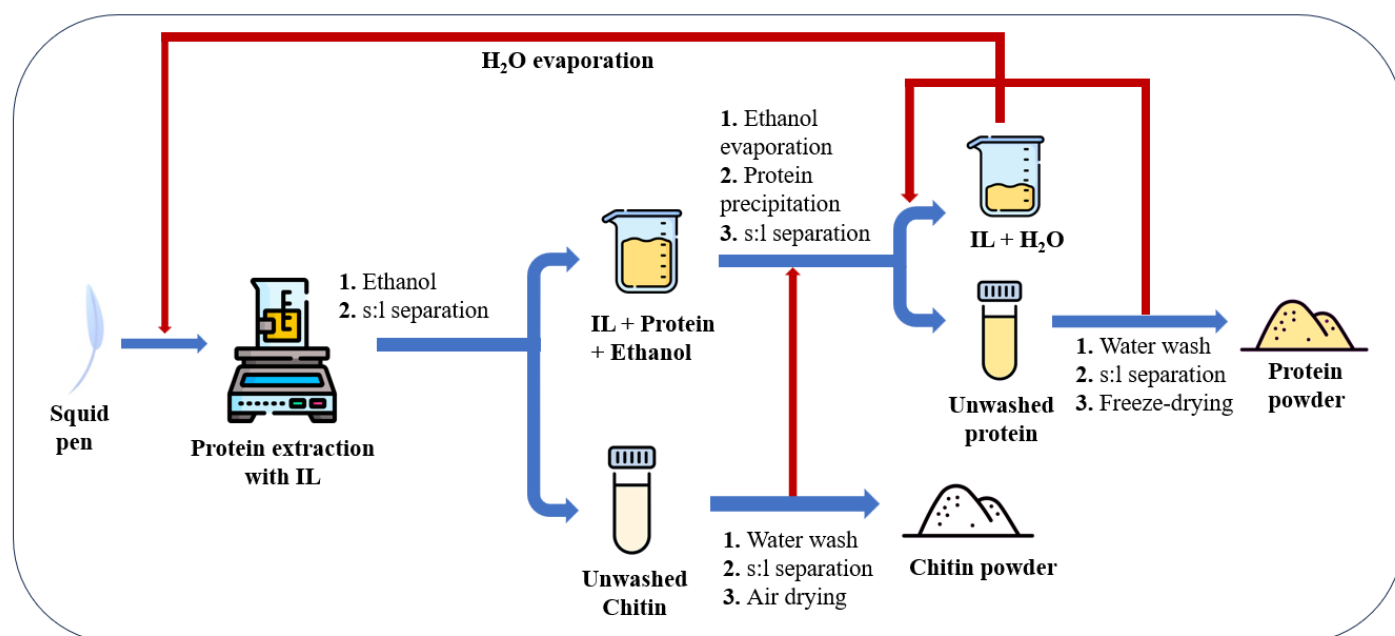
131 **2.4 Optimization of protein extraction for [Ch][OAc]**

132 Once [Ch][OAc] was chosen as the best IL for protein extraction, the optimization of the extraction
133 parameters consisted of three series of experiments: 1) design of experiments (DoE): a 2³+3 (center
134 points) factorial design; 2) single variable experiments for water content and extraction time. The main

135 goal of these experiments was to attain high yield and purity of the squid protein while also producing
136 a high purity β -chitin. A complete description of the experiments can be found in the ESI (Section X).

137 2.5 Recycling of [Ch][OAc]

138 Once protein extraction had been optimized, an IL recycling experiment was performed. The protein
139 extraction was performed at 100 °C, 10 wt% solids loading, 20 wt% water content, and 2 h. The main
140 difference from the previous experiments was that the wash water fractions from the β -chitin and protein
141 were used to precipitate the protein and then added back to the aqueous IL respectively (Figure 1). The
142 IL underwent recycling for five iterations, totalling six cycles in all.



143 **Figure 1.** Recycling of [Ch][OAc] used for squid pen protein extraction. The red arrows correspond
144 to the recycling changes in the IL and wash water fractions.

145 2.6 Material characterization - Analytical Methods

146 Once the β -chitin and protein were obtained under the optimized conditions with [Ch][OAc] — 100
147 °C, 2 h, 5 wt% solids loading and 20 wt% water — a comprehensive material characterization was
148 performed to better understand the two streams that were produced. Details regarding the statistical
149 analyses and analytical procedures for the characterization techniques ¹H-NMR, FT-IR, TGA, SEM,
150 XRD, SDS-PAGE, CHN analysis, amino acid profiling can be found in the ESI (section X).

151 2.7 MD simulations

152 Equilibrium molecular dynamics simulations were conducted utilizing GROMACS 2018.3 CUDA^{26,27}
153 to explore the enhanced efficiency of protein extraction from squid pen by ILs based on acetate and
154 choline. The model protein used was ubiquitin. Initial systems were prepared with 3.0 mol·L⁻¹ IL
155 aqueous solution boxes generated via Packmol^{28,29}. These systems comprised ILs formed by the
156 combination of choline ([Ch]⁺), monoethanolammonium ([MEA]⁺), acetate ([OAc]⁻), and
157 methanesulfonate ([MeSO₃]⁻) ions. Additional information regarding the simulations can be found in
158 the ESI (section X).

159 **2.8 Techno economic analysis**

160 Aspen Plus v11 was employed for process simulation to estimate economic costs and the environmental
161 impact of removing ethanol and water from the IL for its reuse. This was done following similar
162 methodologies reported previously^{21,37}. Additional information regarding the simulations can be found
163 in the ESI (section X).

164 **3. Results and Discussion**

165 **3.1 Chemical composition of squid pen**

166 The chemical composition of the squid pens on a dry basis is: 30 ± 1.3 wt% chitin, 68.6 ± 2.6 wt%
167 protein, 0.5 ± 0.02 wt% ash and 1.1 ± 0.26 wt% lipids. These values are quite similar to those obtained
168 for the composition of *Ilex argentinus*' squid pen by Cortizo et al. (2008)⁴³ with 31 wt% of chitin, 64
169 wt% of protein, 1.0 wt% ash and 2.3 wt% lipids. Additionally, Kurita et al. (1993)⁴⁴ also found similar
170 values for the squid pens of *Ommastrephes bartrami*, 35–40 wt% chitin and 58 wt% of protein. Squid
171 pens are a relatively simple shellfish waste due to its composition, consisting mainly of proteins and
172 chitin.

173 **3.2 IL screening for protein extraction**

174 Acid-base ratio characterisation of the ILs employed in the screening is depicted in Table S15 in the
175 ESI. The ILs present acid-base ratios close to 1.00:1.00, from which, most present acid-base ratios
176 slightly lower than 1, from 0.95 to 0.99, except [Ch][MeSO₃] with 1.07:1.00. Some interesting trends

177 related with the relationship between the pH of the ILs and protein removal can be found by inspecting
178 Fig. 2. From the three acidic ILs — [MEA][HSO₄], [Ch][HSO₄] and [Ch][MeSO₃] — only the [HSO₄]
179 ILs were able to remove the protein from the biomass. The explanation relies on the amount of acidic
180 protons available in the medium. Acidic ILs with [HSO₄]⁻ anions present a high pool of protons
181 available for exchange. In a study by Firth et al. (2024)⁴⁵, they showed through DFT (Density Function
182 Theory) calculations that spontaneous proton dissociation from [HSO₄]⁻ to water occurred for
183 ammonium-based protic ILs, preceded by the formation of an anion trimer structure. Whereas with
184 [Ch][MeSO₃], the slight excess of methane sulfonic acid did not provide sufficient acidity to the system.
185 Although the proteins were removed from the squid pen, the protein yield was near zero because the
186 proteins most likely were hydrolysed in the acidic media. The neutral IL, [MEA][MeSO₃], was also
187 inefficient in promoting any protein solubilisation. And lastly, the alkaline ILs [Ch][OAc] and
188 [MEA][OAc] were able to extract a considerable amount of protein. However, upon anti-solvent
189 addition to the protein-[Ch][OAc] mixture, instantaneous protein precipitation occurred (Video S1 on
190 the ESI), which confirms the superiority of this IL towards protein extraction and recovery. Of course,
191 the pH trend does not solely explain the protein solubility and precipitation; other phenomena related
192 to ion hydrophilicity, intermolecular-interactions and effect of cosolvent which will ultimately impact
193 on the salting-in and out effects of the IL will be covered in section 3.5 with the MD simulations.

194

195

196

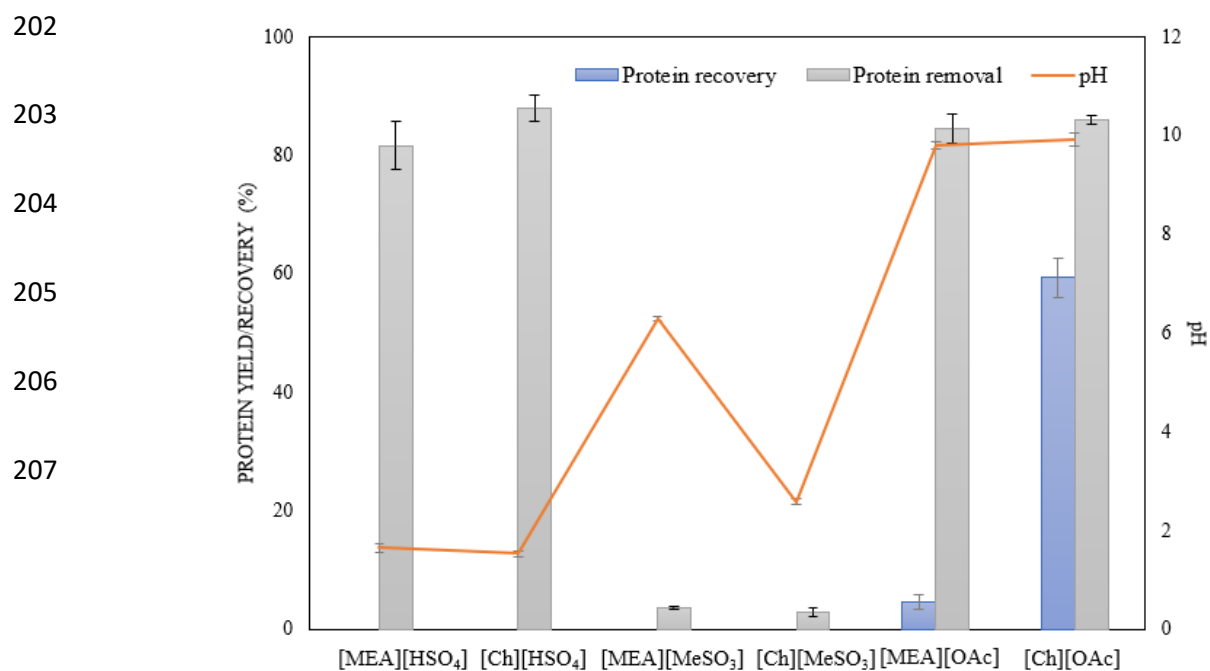
197

198

199

200

201



208 **Figure 2.** IL screening of squid protein extraction: protein removal, recovery, and pH of the IL solution.

209 3.3 Optimisation of protein extraction for [Ch][OAc]

210 Once [Ch][OAc] was chosen, optimisation of the protein extraction parameters was performed.
 211 Extraction time, solids loading, and temperature were chosen as optimisation variables, and two main
 212 response variables were assessed: protein removal and protein yield. Protein extraction experiments
 213 performed under 100 °C did not yield any measurable amount of recovered protein. It can be argued
 214 that high temperatures are necessary to disrupt both the hydrogen bonding and covalent bonds between
 215 protein and chitin. In fact, past studies employed harsh conditions with 1M NaOH under high
 216 temperatures (< 80 °C) at prolonged times to fully remove proteins from squid pens^{9,10,14}. Sodium
 217 hydroxide is a much stronger alkali than [Ch][OAc] due to the presence of hydroxide anions in solution.
 218 Therefore, protein-chitin bond disruption can occur from 80 °C.

219 A new 2² design (with only time and solids loading as parameters) was then extracted from the previous
 220 2³ DoE, with three extra centre point triplicates being added, 10wt% solids loading and 3 h extraction
 221 time. The DoE analysis (ESI) showed that all parameters are significant, including time and temperature
 222 interaction. The statistical significance of the model term coefficients, ANOVA, and Pareto chart for
 223 both protein recovery and removal were shown in the ESI. The analysis showed that all of the model

224 terms are statistically significant ($p < 0.05$). The first-order model fit to the experimental data predicts
225 the response using the following equation:

226
$$\text{Protein removal (\%)} = 79.73 + 19.02T - 28.63S + 14.32 TS \quad (3)$$

227
$$\text{Protein recovery (\%)} = 44.80 - 28.09T - 33.13S + 33.8TS \quad (4)$$

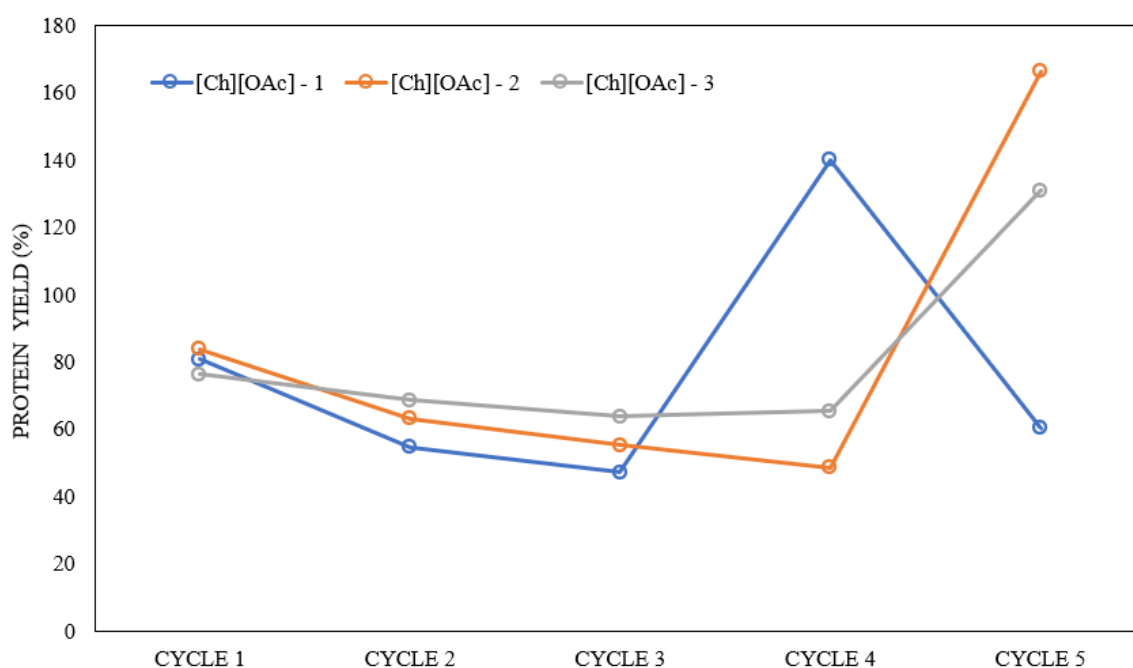
228 Where T and S correspond to the time and solids loading factors (dummy coded, i.e., from -1 to +1),
229 and the R^2 values for the protein removal and recovery were 0.99 and 0.70, respectively, indicating that
230 the efficiency of protein removal is better predicted than how much protein is precipitated. Logically,
231 protein removal is a simpler outcome variable as it only depends on the mass of the samples before and
232 after protein extraction. On the other hand, protein recovery is more complex because it involves both
233 protein removal and their salting out via anti-solvent addition. The surface response plots were shown
234 in Fig. S3 (ESI). Protein removal was favoured by long extraction times and low solids loadings.

235 Alternatively, protein recovery was favoured by low solids and low extraction times. Long extraction
236 times promote protein breakdown into oligopeptides, peptides and amino acids, which may have
237 remained in the IL even upon anti-solvent addition. A compromise between high protein removal and
238 protein recovery must be achieved. A time course experiment (Fig. S6 ESI) showed 2 h of extraction
239 was sufficient to ensure high protein yields ($> 60\%$). Therefore, an extraction time of 2 h and 5 wt%
240 solids loading was chosen as the optimised condition. However, one last parameter needed assessment
241 — the water content of the IL. The protein recovery as a function of the water content can be seen in
242 Fig. S7 (ESI). A water content of lower than 5% was difficult to achieve by rotary evaporation due to
243 the high hydrophilicity of [Ch][OAc], thus the initial water content was 10 wt%. Protein recovery
244 remained high under a low water content, then decreased upon the addition of water to 60% protein
245 recovery with a 40% water content. A higher water content promotes the salting out of the protein and
246 therefore decreases the ionic liquid/protein interactions. As there were no significant differences
247 (section 4.2 from ESI) between a 10 and 20% water content, 20% was chosen as optimal for the IL
248 recycling experiments. A higher water content in the IL decrease the cost related to solvent removal,

249 once [Ch][OAc] is synthesised via diluted aqueous solutions of either [Ch][OH] (46 wt%) or
250 [Ch][HCO₃] (80 wt%).

251 3.4 IL recycling – protein build-up

252 Recycling of [Ch][OAc] was carried out for three samples along five cycles, and the protein recovery
253 yields are reported in Figure 3. It is noticeable that the protein recovery drops after the first cycle to
254 nearly 50% for sample 1 on the third cycle, showing a possible decrease in efficiency. However, the
255 yields sharply increase on the subsequent cycles up to 160%, which suggests that the proteins
256 accumulate in [Ch][OAc] and after a certain threshold, they precipitate back. Sample 1 spiked earlier
257 than the other two samples possibly due to a lower protein recovery on cycles 1-3, which resulted in a
258 higher amount of protein accumulating.



259

260 **Figure 3.** Protein recovery as a function of [Ch][OAc] recycling.

261 Although there has been a significant number of studies on ionic liquid or deep eutectic solvent (choline-
262 chloride based) extraction of proteins^{46,47}, there is still a great gap in the investigation of their recovery
263 and reuse, which poses difficulty to establish comparisons with other approaches. However, similar
264 behavior can be observed in the lignin accumulation during the recycling of trialkyl ammonium

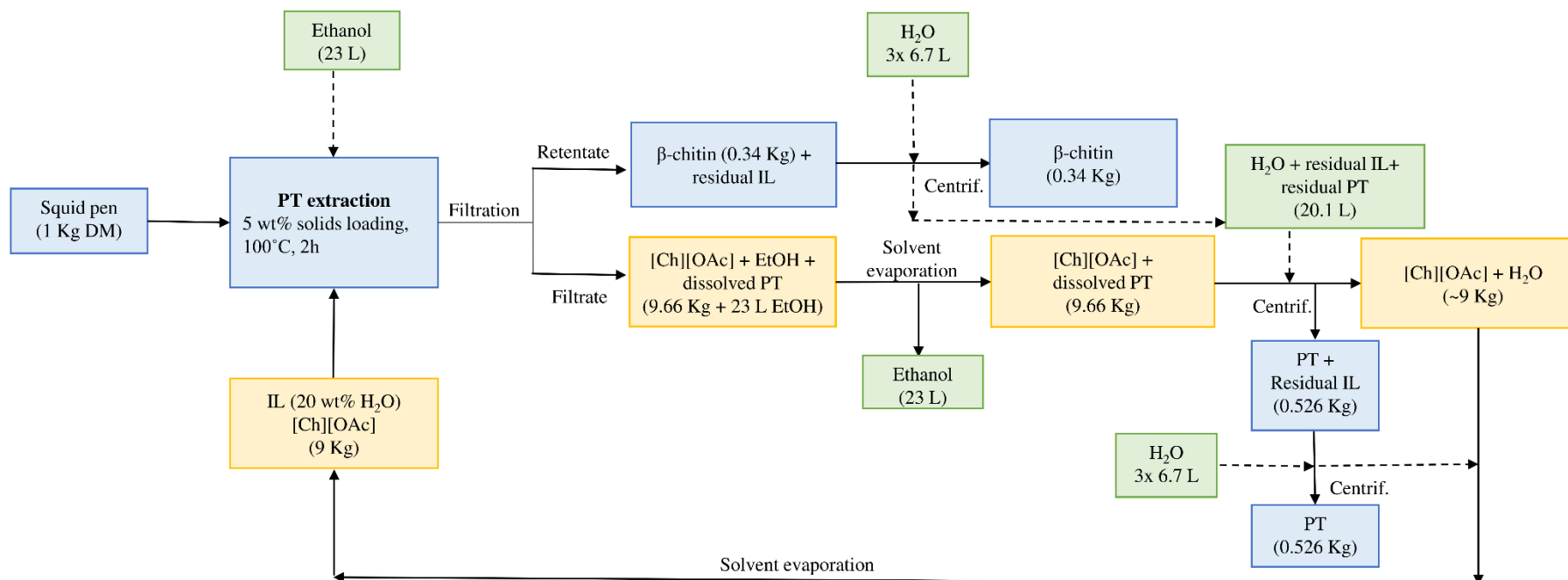
265 hydrogen sulfate IL fractionation of lignocellulosic biomass, as observed by Brandt et al. (2017)⁴⁸ and
266 Abouelela et al. (2021)³⁷. Lignin can be salted out from the IL after fractionation upon the addition of
267 excess water, in a similar method to squid proteins obtained in this work. The phenomenon underlying
268 the lignin precipitation can be attributed to lignin cross-condensation along multiple pretreatment
269 cycles⁴⁸ which does not reflect what happened to the protein. However, the addition of water triggers
270 changes in both ionic strength and pH of the medium, two parameters known to impact the solubility
271 of proteins and facilitate the precipitation of amorphous protein aggregates⁴⁹. Lower ionic strength in
272 aqueous choline-based IL systems is known to increase the likelihood of protein aggregation⁵⁰. A
273 continuous process would yield a different protein accumulation pattern in the IL with a steady state
274 being reached, minimizing the likelihood of sudden spikes in protein precipitation.

275 The IL recovery is also shown in Table S13 (see ESI). On average, most of the [Ch][OAc] was
276 recovered with the washing steps of both chitin and protein. The slight losses along the recovery cycles
277 are most likely due to the protein-bound IL via hydrogen bonding and/or electrostatic interactions.
278 Wahlstrom et al. (2017)⁵¹ have shown that residual [Ch][Cl], up to 2.9 wt%, could be still found on the
279 protein concentrate after dialysis on the extraction of Brewer's spent grain protein with the deep eutectic
280 solvent [Ch][Cl]/urea. Polesca et al. (2023)²¹ employed [Ch][OAc] to extract keratin from chicken
281 feathers and managed to recycle the IL for four cycles without major losses in keratin extraction and IL
282 recovery yields above 90 wt%. Nevertheless, they did not observe keratin accumulation on IL along the
283 cycles, which may be related to differences in protein polarity. Once keratin is known to be hydrophobic
284 and more insoluble in solvents due to the high amount of disulfide bonds, salting out with ethanol/water
285 mixtures promoted their full precipitation from the bulk of the IL⁵². The [Ch][OAc] samples along the
286 cycles have shown no signs of contamination (Figure S8 from ESI) on their ¹H-NMR spectra, which
287 shows that no major by-products were produced upon the extraction.

288 **3.5 Mass Balance**

289 When developing a new process, it is essential to track mass flows for better understanding of critical
290 quantities such as biomass fraction yields and solvent usage. The mass balance for the optimised squid
291 pen extraction with [Ch][OAc] is depicted in Figure 4. The β -chitin yield was 0.34 kg·kg⁻¹ of squid pen,

292 which is consistent with values obtained by Chaussard and Domard (2004) — between 30 and 35 wt%
293 — on the conventional extraction of squid protein from squid pens²⁰. Cuong et al. (2016)¹⁴ also
294 managed to obtain 35.8 wt% of chitin from *Loligo chenis* pens via conventional alkaline extraction.
295 McReynolds et al. (2022) and ⁵³ Lv et al. (2023) ⁵⁴ obtained nearly 30 wt% of β-chitin by using the
296 alkaline deep eutectic solvent K₂CO₃/glycerol. Sulthan et al. (2023)⁵⁵ employed the deep eutectic
297 solvent ChCl/malonic acid to obtain nearly 43 wt% of β-chitin. Approximately, 0.53 kg of protein can
298 be produced per kg of dry squid pen, which is a valuable yet multifunctional stream, due to its several
299 amino acids constituents and it can be obtained in a solid form, facilitating its preservation and storage.
300 In terms of solvent consumption, nearly 40 L of water and 23 L of ethanol were employed per kg of dry
301 squid pens, which is still a considerable amount. However, all the solvent streams can be recycled,
302 which does not generate wastewater.



305 **Figure 4.** Mass balance for the optimised extraction of squid pen protein (PT) with [Ch][OAc]. The blue boxes represent the feedstock and fractions streams.

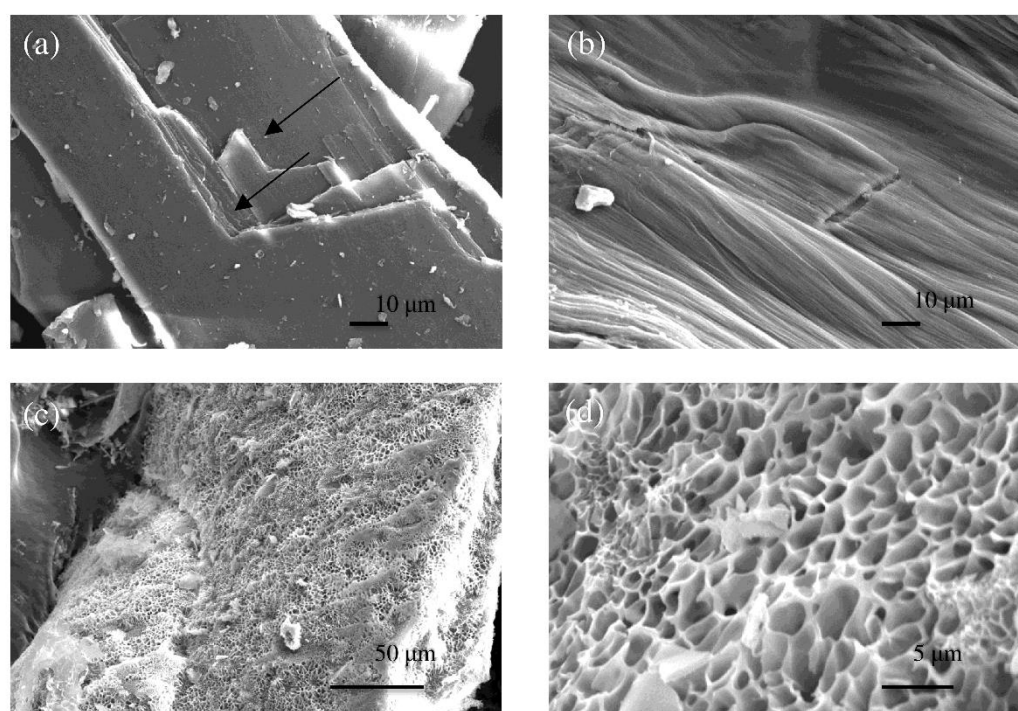
306 The yellow boxes represent the IL streams and the green boxes represent the co-solvent streams. The dashed lines represent the flow of co-solvents.

307 3.6 Materials characterisation summary — β -chitin and protein

308 The extracted β -chitin presents a high degree of acetylation as shown by $^1\text{H-NMR}$ estimation, 94%.
309 This suggests that, despite the use of an alkaline IL, there was insufficient basicity to promote
310 deacetylation of the N-acetyl groups. FT-IR analysis showed the main differences across the samples
311 were related to the relative intensity of the bands. It was noted that the protein and the squid pen (which
312 is mostly composed of proteins) present strong absorptions at 1630 and 1511 cm^{-1} due to the amine
313 bands. Whereas with the β -chitin, even though present—chitin contains N-acetyl groups, which are
314 amides — such bands are lower in intensity. The TGA revealed a trend in which, similarly to the FT-
315 IR spectra, the squid pen had intermediary behavior between the two components (chitin and protein)
316 where T_{onset} for the squid pen was 318 $^{\circ}\text{C}$, for the β -chitin, 326 $^{\circ}\text{C}$, and for the squid protein, 276 $^{\circ}\text{C}$.
317 Additionally, the TGA pattern for the squid pens resembled more of the protein since it is the primary
318 component. The XRD analysis revealed that the CrI of the β -chitin from [Ch][OAc] extraction was
319 higher (82%) than those measured from the conventional extraction method with NaOH (50-70%). The
320 electrophoretic profile of some of the squid proteins obtained in this study showed that the proteins
321 presented similar electrophoretic patterns with two distinct bands, at 10 kDa and between 15 and 25
322 kDa. Such bands are likely to be related to muscular proteins from squid and which are typically present
323 at low molecular weight⁵⁶. The elemental analysis of the protein showed a nitrogen content of $14.4 \pm$
324 0.1% , which corresponds to a protein purity of $90 \pm 0.6\%$, respectively. These values place the
325 [Ch][OAc] fractionation as one of the best to produce high-purity streams from squid waste. The squid
326 protein concentrate obtained in this work had an overall protein content of 43%, excluding tryptophan,
327 which increases to 56% when cysteine and tyrosine are also included. The primary essential amino
328 acids detected were histidine, leucine, and valine, whereas tyrosine, proline, and alanine made up the
329 majority of non-essential amino acids. The biocompatible [Ch][OAc] is a suitable IL choice as the
330 protein isolate can be used for high-protein content feed in aquaculture due to its biocompatibility^{1,57,58}

331 The squid pen surface is slightly rough and is present in layers as visible in Figure 5a. These layers form
332 as a result of the squid's secretion during their formation⁹. Removal of these superficial layers through
333 treatment with [Ch][OAc] reveals a smooth and groovy surface on the β -chitin, as observed in previous

334 studies^{9,59,60}. The freeze-dried squid pen protein is highly porous with nano-sized pores distributed
335 across its surface (Figure 5c-d). These pores were most likely were formed during the freeze-drying
336 process and resemble the formation of hydrogels made of animal protein⁶¹, soy protein⁶² and other
337 biopolymers such as agar⁶², glucomannan⁶³ and modified cellulose⁶⁴.



338 **Figure 5.** SEM surface image of (a) the squid pen; (b) β -chitin after protein extraction with
339 [Ch][OAc]; (c) squid pen protein under low magnification; (d) squid pen protein under high
340 magnification.

341 **3.7 Molecular Dynamics (MD)**

342 The phenomena behind the squid protein extraction with ILs at the molecular level can be quite complex
343 due to the variety of inter- and intramolecular interactions involved. Nevertheless, past studies on the
344 interaction of proteins with ILs have shown cooperative and competitive effects of IL solvation of
345 proteins can be rationalized.^{49,65,66} Squid proteins, especially muscular ones such as actin, myosin, and
346 tropomyosin, are known to thermally denature from 40 °C to 80°C^{9,67,68}. IL treatment at 100 °C most
347 likely caused the squid pen proteins to denature. Bui-le et al.(2020)⁶⁶ have also shown that proteins such
348 as the green fluorescent protein are more easily denatured in the presence of pyrrolidinium-based ILs,

349 which may reinforce that protein denaturation may have happened even below 100 °C, which then
350 caused their unfolding and exposure of the hydrophobic core. The acetate anion presents a high value
351 of the Kamlet-Taft parameter β related to the hydrogen-bond basicity; it is known that high β values
352 may lead to protein destabilization⁴⁹. Once denatured, the protein remains soluble in the IL and upon
353 the addition of ethanol as a co-solvent. After ethanol evaporation and the addition of excess of water,
354 the protein was salted out from the IL due to the stronger IL-water interactions. The goal of these MD
355 simulations was twofold: first, to understand why protein solubilization was more effective in ionic
356 liquids with the [OAc] anion. Second, to rationalize why the combination of [OAc] with the [Ch] cation
357 allows optimal recovery of the proteins.

358 **3.7.1 Anion-protein interactions**

359 Minimum distance distribution functions (MDDFs) for two distinct IL systems sharing the same cation
360 are shown in Figure 6. The MDDFs peaks indicate the regions with the highest probability of locating
361 the compound of interest in the solution relative to the protein surface. The MDDFs for the anions
362 exhibit significant differences in the systems. Specifically, in the [OAc]⁻ MDDF (Figure 6a), a sharp
363 peak appears at ~ 1.9 Å, showing a high probability of acetate-protein hydrogen bonds.^{65,69} Another
364 important [OAc]⁻ MDDF peak appears at ~ 2.9 Å and is a result of van der Waals interactions with the
365 protein or interactions mediated by other ions or water molecules. The position of the cation peak, which
366 intermediates the two anion peaks, suggests alternating charge solvation layers, thus a strong cation-
367 anion cooperative solvation effect. The accumulation of [MeSO₃] in [Ch][MeSO₃] (Fig. 6b) is less
368 pronounced than that of [OAc], being the second peak greater than the first, and both smaller than that
369 of the cation. Clearly, [OAc] is a stronger binding to the protein surface than [MeSO₃].

370

371

372

373

374

375

376

377

378

379

380

381

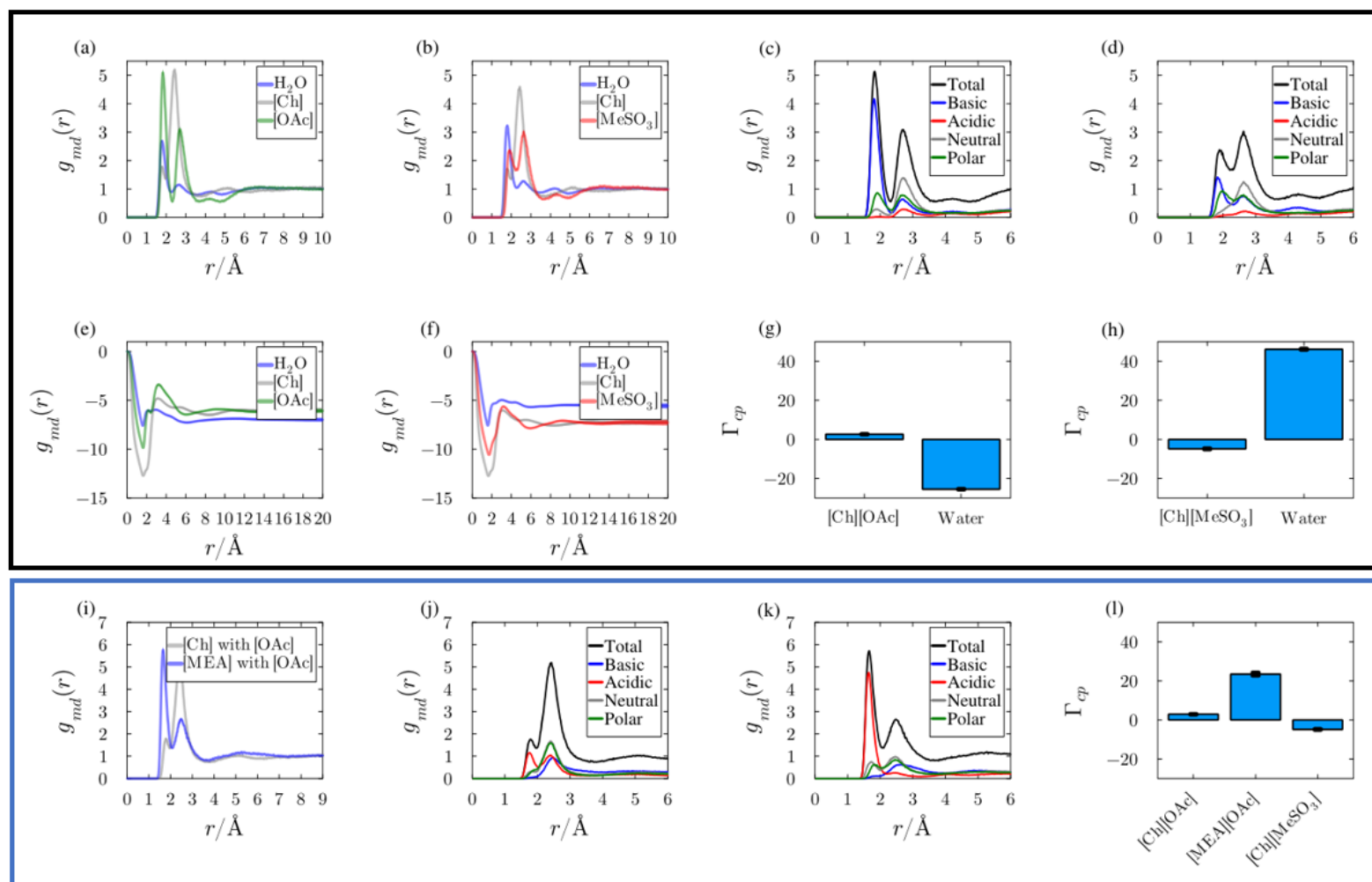


Figure 6. Protein solvation in IL systems using Minimum Distance Distribution Functions (MDDFs) and the Kirkwood-Buff (KB) theory of solvation. The figures enclosed in the black box show the distributions and KB-integrals of the anions [OAc]⁻ and [MeSO₃]⁻ in the presence of the same cation. The figures enclosed in the blue box refer to the distributions of the cations [Ch]⁺ and [MEA]⁺ in the presence of a shared anion. Panels (a) and (b) illustrate the MDDFs for of [Ch] and [OAc] and of [Ch] and [MeSO₃], respectively. Panels (c) and (d) show a stronger association with basic residues, particularly for [OAc]⁻. Panels (e) and (f) present the KB integrals for both IL systems, and panels (g) and (h) compare the preferential solvation parameters. Panels (i) to (k) offer a comparative analysis of protein solvation using the [OAc]⁻ anion with [Ch]⁺ and [MEA]⁺ cations. Finally, Panel (l) contrasts the preferential solvation parameters between ILs with different cations, underscoring the variance in solvation preference and interaction strengths within these complex systems.

382 Protein residue-type contributions for the total MDDF distribution of ions are displayed in
383 Figures 6c and 6d. In Figure 6a, the first peak of the MDDF of $[\text{OAc}]^-$ results from interactions with
384 basic protein residues, mediated by interactions with the acetate oxygen (ESI, Figure S5). In contrast,
385 $[\text{MeSO}_3]^-$ exhibits a smaller relative probability of interactions with basic residues than $[\text{OAc}]^-$. One
386 can note, in Figure 6d the MDDF shows significant interactions with basic residues at hydrogen-
387 bonding distances; however, such contribution to the total MDDF is also smaller than specific
388 interactions displayed by the $[\text{OAc}]^-$ anion.

389 Kirkwood-Buff Integrals (KBIs) for the $[\text{Ch}][\text{OAc}]$ and $[\text{Ch}][\text{MeSO}_3]$ IL systems are shown in
390 Figure 6. In brief, when the water KBI exceeds that of the ions, it indicates a greater relative affinity of
391 water for the protein surface. In the case of acetate, the ions' KBIs exhibit a stronger affinity for the
392 protein surface, whereas for $[\text{MeSO}_3]^-$, the opposite trend is observed. This means that the IL with
393 $[\text{OAc}]^-$ preferentially solvates the protein relative to water, while the protein is preferentially hydrated
394 when the anion is $[\text{MeSO}_3]^-$, as shown in Figures 6c and 6d. The greater preferential solvation parameter
395 implies that a greater number of IL ions is found around the protein for the system with $[\text{Ch}][\text{OAc}]$ than
396 with $[\text{Ch}][\text{MeSO}_3]$, for the same bulk concentration. In general, solutes that dehydrate proteins induce
397 protein denaturation and may facilitate protein solubilization, as the protein tends expose its surface to
398 the solution.

399 3.7.2 Cation-protein interactions

400 The distributions of components in solutions with different cations, but sharing the same anion are
401 shown in Figure 6(i-k). The shared anion is $[\text{OAc}]^-$ and either $[\text{MEA}]^+$ or $[\text{Ch}]^+$ are the cations. The
402 distributions of $[\text{Ch}]^+$ (in gray) and $[\text{MEA}]^+$ (in blue) display two primary peaks at approximately 1.8
403 Å, resulting of hydrogen bonds formed with the protein's surface. While both cations exhibit MDDFs
404 with two peaks within 5 Å of the protein surface, the first peak is notably more pronounced for $[\text{MEA}]^+$.
405 This suggests a higher likelihood of $[\text{MEA}]^+$ forming hydrogen bond interactions with the protein,
406 particularly with acidic residues (Figure 6k). This significant contribution from acidic residues is not
407 observed when the cation is $[\text{Ch}]^+$, as shown in Figure 6j. The inability of $[\text{MEA}]^+$ to induce protein
408 precipitation, despite its solubilization capability, might be inferred from Figure 6l: Both ionic liquids

409 (ILs) with these cations preferentially solvate the protein, and thus interact favourably with the protein
410 surface relative to water. Yet, the preferential solvation by [MEA]⁺ is significantly stronger than for
411 [Ch]⁺. This potentially explains difficulty in precipitating the protein from the solutions with [MEA]⁺.
412 While the IL containing [Ch]⁺ also preferentially solvates proteins when compared to water, its
413 comparative affinity to the protein surface is much weaker than that of [MEA]⁺, thereby facilitating
414 protein recovery.

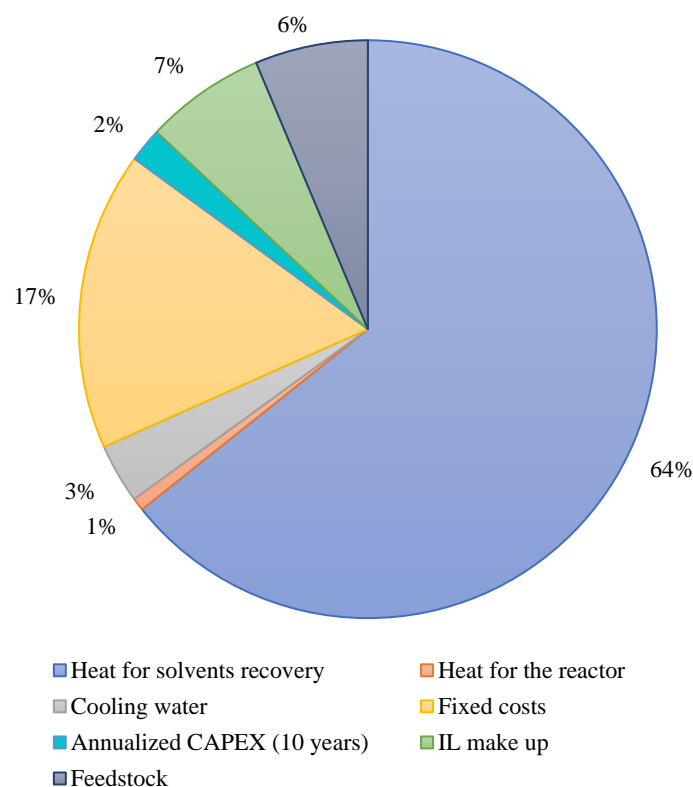
415

416 **3.8 Techno-economic analysis**

417 Techno-economic was conducted to evaluate the effects of the protein extraction process. These
418 assessments are particularly crucial to minimise solvent consumption for environmental and economic
419 issues, as ethanol and water are introduced at various stages of the process to facilitate the recovery of
420 chitin and protein. Consequently, energy is required for the evaporation of these substances to achieve
421 the appropriate composition for the recovery of ionic liquid (IL) for reuse. The IL recovery was set to
422 97%, following previous results shown in Table S13 (ESI). In addition, the experimental values reported
423 in Figure 4 were considered for the estimation of heat consumption for ethanol and water evaporation.

424 The simulation takes into account heating the squid pen and IL mixture up to 100°C for protein
425 extraction. Then, ethanol evaporation was simulated by a flash vessel at 0.1 bar, optimized by trial and
426 error until no ethanol was detected in the bottom stream (IL + water). No IL was recovered in the top
427 stream. 1.1 kg water·kg⁻¹ of IL as low-pressure steam was necessary to provide the heat needed for the
428 distillation. The top stream (ethanol) was condensed and then cooled to room temperature and
429 recirculated, recovering the excess heat for its employment in the subsequent separations. Two-step
430 multiple-effect evaporators were used for water removal and IL recovery. Pressure in both vessels (0.3
431 and 0.1 bar in the first and second vessel, respectively) was optimized by trial and error to minimize
432 vacuum and energy consumption and ensure the recovered IL matched the required characteristics for
433 its reuse. The excess heat from ethanol condensation was used in the first step, as well as an additional
434 1.78 kg water·kg⁻¹ of IL as low-pressure steam for heating needs. Excess heat from water condensation

435 in the top of the vessel was recovered and employed in the second step, with no additional heating
436 needs. Water was cooled down to room temperature and recirculated. IL was then heated up again to
437 100°C and recirculated. From the simulation, annual costs were calculated as described in the
438 methodology section; their percentual contribution to the minimum protein selling price is depicted in
439 Fig. 7. Electricity contribution (due to pumping) is not shown as it accounted for less than 0.2%.



440

441

Figure 7. Percentual contributions to the minimum protein selling price.

442 As expected, the most significant contribution is the heat needed for solvent recovery due to the high
443 volumes of ethanol and, mainly, water (85 wt% after mixing with the IL) employed in the process. This
444 is especially important considering the heat of vaporization of water is 2.65 times higher than that for
445 ethanol. For this, energy consumption in the multiple-effect evaporators for water evaporation is 1.6
446 times higher than for ethanol removal, accounting for 40% of the minimum protein selling price.
447 Therefore, new methods for IL recovery are worth investigating to improve the energy efficiency of the
448 process. IL makeup costs were calculated considering a 97% IL recovery from experimental results in
449 laboratory, which may not completely translate to a larger scale⁷⁰. The large volumes of solvents

450 employed for relatively low productivity lead to high total field costs (due to equipment), which impacts
451 the fixed costs, significantly contributing to the minimum selling price. The main contribution to these
452 costs is the three evaporators employed in ethanol and water distillations, accounting for 15% of all
453 fixed costs. Finally, it is important to note that feedstock costs are estimated using a squid pen powder
454 price that may not be current, given the challenge of accessing updated pricing information. Hence,
455 caution is advised in considering this aspect, as there is potential for cost reduction if the plant is
456 integrated into the fish industry, where squid pens are commonly viewed as a waste material.

457 According to our simulation and considering all the costs explained in the methodology section, the
458 minimum protein selling price obtained is 9 \$·kg⁻¹, which was calculated considering a protein
459 productivity of 416 ton/year, in accordance with the mass balance (Fig. 4) for simulated flow rates.
460 However, it is worth mentioning that this price was calculated considering only protein and does not
461 take into account the possible income from selling β-chitin as a by-product. Thus, based on chitin
462 productivity and considering a price of 3.75 \$·kg⁻¹, the protein selling price could be lowered to
463 approximately 6.6 \$·kg⁻¹. In terms of environmental impact, the process generates CO₂ emissions of
464 4.27 kg CO₂·kg⁻¹ of products, factoring in the production of both protein and β-chitin, which account
465 for 61% and 39% of CO₂ emissions, respectively. The predominant source of these CO₂ emissions is
466 the significant energy requirements of the solvent recovery process, compounded by the limited
467 availability of heat sources beyond steam. This underscores the critical need to explore alternative
468 methods for recovering ILs from water streams, given their substantial impact on both economic and
469 environmental considerations. A more flexible method for IL dehydration is pervaporation, a scalable
470 membrane separation technique that can be selective toward the direct recovery of volatile solutes or
471 solvents from non-volatile solvents in a quantitative manner⁷².

472 **4. Conclusions and perspectives**

473 Designing ILs for protein extraction requires appropriate selection of cation and anion combination.
474 Squid pens are an excellent model for a shellfish biorefinery because they present more simple
475 composition when compared to crabs, prawns and lobsters. In this work, an ionic-liquid based process
476 with [Ch][OAc] was designed and optimised that can generate two product streams of high purity, squid

477 protein and β -chitin. Recycling of the IL showed that protein accumulates for a number of recycles and
478 can eventually be recovered, without compromising the efficiency and purity of the IL. The mass
479 balance of the process revealed that the solvent usage is high, however, process integration and IL
480 recycling can ensure greener credentials for the process. Material characterisation of the two streams
481 showed that the β -chitin presents a low protein content and is highly crystalline, whereas and the protein
482 isolate has a high protein content and low molecular weight. Although it can be directed towards β -
483 chitosan production — which would add an additional environmental burden due to its high waste
484 generation⁷³ — β -chitin can be electrospun into scaffolds or mats for biomedical applications such as
485 wound dressings, drug delivery agents or bone-growth scaffolds^{74,75}. For instance, Gomes et al. (2020)⁷⁶
486 employed the same IL used in this study, [Ch][OAc], to produce biocompatible, highly porous, and
487 interconnected sponges from crab shells α -chitin. Biocompatibility was probed by assessing the
488 metabolic activity of L929 fibroblasts and seeding human adipose stem cells on the sponge surface.
489 Despite a solvent intensive synthesis, chitin nano whiskers have been employed as reinforcing agents
490 in elastomers synthesis, either in epoxidized natural rubber⁷⁷, in elastomeric composites with
491 polycaprolactone⁷⁸ or modified polyurethanes⁷⁵.

492 Amino acid profiling of the protein isolate showed that the major essential amino acids were histidine,
493 leucine and valine, which can be a source of valuable amino acids for aqua culture^{57,58} and applications
494 in human feed is also a potential avenue^{56,79}. Nonetheless, caution needs to be taken regarding
495 allergenicity triggered by tropomyosin⁸⁰. MD simulations unveiled the reasoning behind the superiority
496 of [Ch][OAc] to extract and precipitate protein from aqueous solutions, in comparison to other ILs
497 screened with the same cation or anion, underpinning the role of the anion on the protein extraction and
498 the role of the cation on the protein precipitation. Techno-economic analysis showed how energetic
499 requirements for washing steps and IL recovery can heavily impact on the protein minimum selling
500 price. The co-production of β -chitin decreases the minimum selling price of the protein. Solvent usage
501 impacts negatively on CO₂ emissions and emphasizes that despite its promise, an IL-based refinery
502 requires further design process integration and optimised heat recovery, as well as increased efficiency
503 in separation processes. This work can be viewed as the foundation of an IL-based biorefinery for

504 shellfish., where future works on carbonate-rich shellfish such as crabs, prawns and lobster can be
505 beneficial for the holistic utilization of shellfish waste.

506 6. Acknowledgements

507 This work was partially supported by the São Paulo Foundation for Research (FAPESP) grants
508 2018/24293-0, [2013/08293-7](#), and 2023/02167-1. The authors also wish to acknowledge Mark
509 Richardson, and the Engineering and Physical Sciences Research Council and the Supergen Bioenergy
510 Hub — EP/Y016300/1 — for supporting this work.

511 7. References

512

- 513 1. Cooney R, de Sousa DB, Fernández-Ríos A, et al. A circular economy framework for seafood
514 waste valorisation to meet challenges and opportunities for intensive production and
515 sustainability. *J Clean Prod.* 2023;392:136283. doi:10.1016/j.jclepro.2023.136283
- 516 2. Miller N. Data advances understanding of global squid fishing fleets.
517 <https://globalfishingwatch.org>. March 2023. Accessed October 19, 2023.
518 <https://globalfishingwatch.org/data/data-advances-understanding-global-squid-fishing-fleets/>
- 519 3. Venugopal V. Green processing of seafood waste biomass towards blue economy. *CRSUST.*
520 2022;4:100164. doi:10.1016/j.crsust.2022.100164
- 521 4. Denéchère R, van Denderen PD, Andersen KH. The role of squid for food web structure and
522 community-level metabolism. *BioRxiv.* July 18, 2023. doi:10.1101/2023.07.14.549083
- 523 5. Clark J, Deswarte F. The biorefinery concept: an integrated approach. In: Clark J, Deswarte F,
524 eds. *Introduction to Chemicals from Biomass.* Wiley; 2015:1-29.
525 doi:10.1002/9781118714478.ch1
- 526 6. Zeidberg LD, Robison BH. Invasive range expansion by the Humboldt squid, *Dosidicus gigas*,
527 in the eastern North Pacific. *Proc Natl Acad Sci USA.* 2007;104(31):12948-12950.
528 doi:10.1073/pnas.0702043104
- 529 7. Wang C-H, Doan CT, Nguyen AD, Wang S-L. Reclamation of Fishery Processing Waste: A
530 Mini-Review. *Molecules.* 2019;24(12). doi:10.3390/molecules24122234
- 531 8. Yan N, Chen X. Sustainability: Don't waste seafood waste. *Nature.* 2015;524(7564):155-157.
532 doi:10.1038/524155a
- 533 9. Messerli MA, Raihan MJ, Kobylkevich BM, et al. Construction and Composition of the Squid
534 Pen from *Doryteuthis pealeii*. *Biol Bull.* 2019;237(1):1-15. doi:10.1086/704209
- 535 10. Yang F-C, Peters RD, Dies H, Rheinstädter MC. Hierarchical, self-similar structure in native
536 squid pen. *Soft Matter.* 2014;10(30):5541-5549. doi:10.1039/c4sm00301b

- 537 11. Shavandi A, Hu Z, Teh S, et al. Antioxidant and functional properties of protein hydrolysates
538 obtained from squid pen chitosan extraction effluent. *Food Chem.* 2017;227:194-201.
539 doi:10.1016/j.foodchem.2017.01.099
- 540 12. Nguyen TT, Heimann K, Zhang W. Protein Recovery from Underutilised Marine Bioresources
541 for Product Development with Nutraceutical and Pharmaceutical Bioactivities. *Mar Drugs.*
542 2020;18(8). doi:10.3390/md18080391
- 543 13. Krishnan S, Chakraborty K, Dhara S. Biomedical potential of β -chitosan from cuttlebone of
544 cephalopods. *Carbohydr Polym.* 2021;273:118591. doi:10.1016/j.carbpol.2021.118591
- 545 14. Cuong HN, Minh NC, Van Hoa N, Trung TS. Preparation and characterization of high purity
546 β -chitin from squid pens (*Loligo chenis*). *Int J Biol Macromol.* 2016;93(Pt A):442-447.
547 doi:10.1016/j.ijbiomac.2016.08.085
- 548 15. Abdelmalek BE, Sila A, Haddar A, Bougatef A, Ayadi MA. β -Chitin and chitosan from squid
549 gladius: Biological activities of chitosan and its application as clarifying agent for apple juice.
550 *Int J Biol Macromol.* 2017;104(Pt A):953-962. doi:10.1016/j.ijbiomac.2017.06.107
- 551 16. Riofrio A, Alcivar T, Baykara H. Environmental and Economic Viability of Chitosan
552 Production in Guayas-Ecuador: A Robust Investment and Life Cycle Analysis. *ACS Omega.*
553 2021;6(36):23038-23051. doi:10.1021/acsomega.1c01672
- 554 17. Nakasu PYS, Verdía Barbará P, Firth AEJ, Hallett JP. Pretreatment of biomass with protic
555 ionic liquids. *Trends in Chemistry.* 2022;4(3):175-178. doi:10.1016/j.trechm.2021.12.001
- 556 18. de Jesus SS, Maciel Filho R. Are ionic liquids eco-friendly? *Renew Sustain Energy Rev.*
557 2022;157:112039. doi:10.1016/j.rser.2021.112039
- 558 19. Shamshina JL, Abidi N. Isolation of Chitin Nano-whiskers Directly from Crustacean Biomass
559 Waste in a Single Step with Acidic Ionic Liquids. *ACS Sustain Chem Eng.* 2022;10(36):11846-
560 11855. doi:10.1021/acssuschemeng.2c02461
- 561 20. Chaussard G, Domard A. New aspects of the extraction of chitin from squid pens.
562 *Biomacromolecules.* 2004;5(2):559-564. doi:10.1021/bm034401t
- 563 21. Polesca C, Al Ghatta A, Passos H, Coutinho JAP, Hallett JP, Freire MG. Sustainable keratin
564 recovery process using a bio-based ionic liquid aqueous solution and its techno-economic
565 assessment. *Green Chem.* 2023;25(10):3995-4003. doi:10.1039/D3GC00850A
- 566 22. Nakasu PYS, Clarke CJ, Rabelo SC, Costa AC, Brandt-Talbot A, Hallett JP. Interplay of acid-
567 base ratio and recycling on the pretreatment performance of the protic ionic liquid
568 monoethanolammonium acetate. *ACS Sustain Chem Eng.* 2020;8(21):7952-7961.
569 doi:10.1021/acssuschemeng.0c01311
- 570 23. Pérez-Álvarez L, Ruiz-Rubio L, Vilas-Vilela JL. Determining the deacetylation degree of
571 chitosan: opportunities to learn instrumental techniques. *J Chem Educ.* 2018;95(6):1022-1028.
572 doi:10.1021/acs.jchemed.7b00902
- 573 24. Polesca C, Passos H, Neves BM, Coutinho JAP, Freire MG. Valorization of chicken feathers
574 using aqueous solutions of ionic liquids. *Green Chem.* 2023;25(4):1424-1434.
575 doi:10.1039/D2GC04477C
- 576 25. Hames B, Sluiter A, Scarlata C. *Determination of Protein Content in Biomass. Laboratory*
577 *Analytical Procedure (LAP).* Vol NREL/TP; 510-42625. National Renewable Energy
578 Laboratory; 2008.

- 579 26. Van Der Spoel D, Lindahl E, Hess B, Groenhof G, Mark AE, Berendsen HJC. GROMACS:
580 fast, flexible, and free. *J Comput Chem.* 2005;26(16):1701-1718. doi:10.1002/jcc.20291
- 581 27. Kohnke B, Ullmann RT, Kutzner C, et al. A Flexible, GPU - Powered Fast Multipole Method
582 for Realistic Biomolecular Simulations in Gromacs. *Biophys J.* 2017;112(3):448a.
583 doi:10.1016/j.bpj.2016.11.2402
- 584 28. Martínez L, Andrade R, Birgin EG, Martínez JM. PACKMOL: a package for building initial
585 configurations for molecular dynamics simulations. *J Comput Chem.* 2009;30(13):2157-2164.
586 doi:10.1002/jcc.21224
- 587 29. Martínez JM, Martínez L. Packing optimization for automated generation of complex system's
588 initial configurations for molecular dynamics and docking. *J Comput Chem.* 2003;24(7):819-
589 825. doi:10.1002/jcc.10216
- 590 30. Robertson MJ, Tirado-Rives J, Jorgensen WL. Improved Peptide and Protein Torsional
591 Energetics with the OPLSAA Force Field. *J Chem Theory Comput.* 2015;11(7):3499-3509.
592 doi:10.1021/acs.jctc.5b00356
- 593 31. Jorgensen WL, Chandrasekhar J, Madura JD, Impey RW, Klein ML. Comparison of simple
594 potential functions for simulating liquid water. *J Chem Phys.* 1983;79(2):926.
595 doi:10.1063/1.445869
- 596 32. Darden T, York D, Pedersen L. Particle mesh Ewald: An N-log(N) method for Ewald sums in
597 large systems. *J Chem Phys.* 1993;98(12):10089. doi:10.1063/1.464397
- 598 33. Bezanson J, Edelman A, Karpinski S, Shah VB. Julia: A fresh approach to numerical
599 computing. *SIAM Rev.* 2017;59(1). doi:10.1137/141000671
- 600 34. Martínez L. ComplexMixtures.jl: Investigating the structure of solutions of complex-shaped
601 molecules from a solvent-shell perspective. *J Mol Liq.* 2022;347:117945.
602 doi:10.1016/j.molliq.2021.117945
- 603 35. Baynes BM, Trout BL. Proteins in Mixed Solvents: A Molecular-Level Perspective. *J Phys
604 Chem B.* 2003;107(50):14058-14067. doi:10.1021/jp0363996
- 605 36. Martínez L, Shimizu S. Molecular Interpretation of Preferential Interactions in Protein
606 Solvation: A Solvent-Shell Perspective by Means of Minimum-Distance Distribution
607 Functions. *J Chem Theory Comput.* 2017;13(12):6358-6372. doi:10.1021/acs.jctc.7b00599
- 608 37. Abouelela AR, Al Ghatta A, Verdía P, Shan Koo M, Lemus J, Hallett JP. Evaluating the Role
609 of Water as a Cosolvent and an Antisolvent in [HSO₄]⁻-Based Protic Ionic Liquid
610 Pretreatment. *ACS Sustain Chem Eng.* 2021;9(31):10524-10536.
611 doi:10.1021/acssuschemeng.1c02299
- 612 38. Shabani MR, Yekta RB. Chemical processes equipment cost estimation using parametric
613 models. *Cost Engineering.* 2006;48:22-25.
- 614 39. Al Ghatta A, Wilton-Ely JDET, Hallett JP. From sugars to FDCA: a techno-economic
615 assessment using a design concept based on solvent selection and carbon dioxide emissions.
616 *Green Chem.* 2021. doi:10.1039/D0GC03991H
- 617 40. Ovejero-Pérez A, Ayuso M, Rigual V, et al. Technoeconomic Assessment of a Biomass
618 Pretreatment + Ionic Liquid Recovery Process with Aprotic and Choline Derived Ionic
619 Liquids. *ACS Sustain Chem Eng.* 2021;9(25):8467-8476. doi:10.1021/acssuschemeng.1c01361

- 620 41. Wang S-L, Wang C-Y, Yen Y-H, Liang T-W, Chen S-Y, Chen C-H. Enhanced production of
621 insecticidal prodigiosin from *Serratia marcescens* TKU011 in media containing squid pen.
622 *Process Biochemistry*. 2012;47(11):1684-1690. doi:10.1016/j.procbio.2011.07.010
- 623 42. Berger LRR, Stamford TCM, Stamford-Arnaud TM, et al. Green conversion of agroindustrial
624 wastes into chitin and chitosan by *Rhizopus arrhizus* and *Cunninghamella elegans* strains. *Int J*
625 *Mol Sci*. 2014;15(5):9082-9102. doi:10.3390/ijms15059082
- 626 43. Susana Cortizo M, Berghoff CF, Alessandrini JL. Characterization of chitin from *Illex*
627 *argentinus* squid pen. *Carbohydr Polym*. 2008;74(1):10-15. doi:10.1016/j.carbpol.2008.01.004
- 628 44. Kurita K, Tomita K, Tada T, Ishii S, Nishimura S, Shimoda K. Squid chitin as a potential
629 alternative chitin source: Deacetylation behavior and characteristic properties. *J Polym Sci A*
630 *Polym Chem*. 1993;31(2):485-491. doi:10.1002/pola.1993.080310220
- 631 45. Firth AEJ, Nakasu PYS, Hallett JP, Matthews RP. Exploiting cation structure and water
632 content in modulating the acidity of ammonium hydrogen sulfate protic ionic liquids. *J Phys*
633 *Chem Lett*. February 22, 2024;2311-2318. doi:10.1021/acs.jpcclett.3c03583
- 634 46. Nunes JCF, Almeida MR, Faria JL, et al. Overview on Protein Extraction and Purification
635 Using Ionic-Liquid-Based Processes. *J Solution Chem*. 2022;51(3):243-278.
636 doi:10.1007/s10953-021-01062-x
- 637 47. Zhou Y, Wu W, Zhang N, Soladoye OP, Zhang Y, Fu Y. Deep eutectic solvents as new media
638 for green extraction of food proteins: Opportunity and challenges. *Food Res Int*.
639 2022;161:111842. doi:10.1016/j.foodres.2022.111842
- 640 48. Brandt-Talbot A, Gschwend FJV, Fennell PS, et al. An economically viable ionic liquid for
641 the fractionation of lignocellulosic biomass. *Green Chem*. 2017;19(13):3078-3102.
642 doi:10.1039/C7GC00705A
- 643 49. Han Q, Brown SJ, Drummond CJ, Greaves TL. Protein aggregation and crystallization with
644 ionic liquids: Insights into the influence of solvent properties. *J Colloid Interface Sci*.
645 2022;608(Pt 2):1173-1190. doi:10.1016/j.jcis.2021.10.087
- 646 50. Shmool TA, Martin LK, Matthews RP, Hallett JP. Ionic Liquid-Based Strategy for Predicting
647 Protein Aggregation Propensity and Thermodynamic Stability. *JACS Au*. 2022;2(9):2068-
648 2080. doi:10.1021/jacsau.2c00356
- 649 51. Wahlström R, Rommi K, Willberg-Keyriläinen P, et al. High Yield Protein Extraction from
650 Brewer's Spent Grain with Novel Carboxylate Salt - Urea Aqueous Deep Eutectic Solvents.
651 *ChemistrySelect*. 2017;2(29):9355-9363. doi:10.1002/slct.201701492
- 652 52. Shavandi A, Silva TH, Bekhit AA, Bekhit AE-DA. Keratin: dissolution, extraction and
653 biomedical application. *Biomater Sci*. 2017;5(9):1699-1735. doi:10.1039/c7bm00411g
- 654 53. McReynolds C, Adrien A, de Fraissinette NB, Olza S, Fernandes SCM. Deep eutectic solvents
655 for the extraction of β -chitin from *Loligo vulgaris* squid pens: a sustainable way to valorize
656 fishery by-products. *Biomass Conv Bioref*. November 24, 2022. doi:10.1007/s13399-022-
657 03569-9
- 658 54. Lv J, Fang Y, Wang D, et al. Green preparation of β -chitins from squid pens by using alkaline
659 deep eutectic solvents. *Int J Biol Macromol*. 2023;253(Pt 2):126767.
660 doi:10.1016/j.ijbiomac.2023.126767

- 661 55. Sulthan R, Sambhudevan S, Greeshma S, et al. Extraction of β -chitin using deep eutectic
662 solvents for biomedical applications. *Materials Today: Proceedings*. 2023;94:44-48.
663 doi:10.1016/j.matpr.2023.05.521
- 664 56. Omote-Sibina JR, Roldán-Acero DJ. Identification of soluble proteins present in giant squid
665 (*Dosidicus gigas*) meal for human consumption. *Agron Mesoam*. January 17, 2023:50264.
666 doi:10.15517/am.v34i2.50264
- 667 57. Xing S, Liang X, Zhang X, et al. Essential amino acid requirements of fish and crustaceans, a
668 meta-analysis. *Rev Aquacult*. December 14, 2023. doi:10.1111/raq.12886
- 669 58. Boyd CE, McNevin AA, Davis RP. The contribution of fisheries and aquaculture to the global
670 protein supply. *Food Sec*. 2022;14(3):805-827. doi:10.1007/s12571-021-01246-9
- 671 59. Montroni D, Sparla F, Fermani S, Falini G. Influence of proteins on mechanical properties of a
672 natural chitin-protein composite. *Acta Biomater*. 2021;120:81-90.
673 doi:10.1016/j.actbio.2020.04.039
- 674 60. Balitaan JN, Martin GAV, Santiago KS. Revamping squid gladii to biodegradable
675 composites: In situ grafting of polyaniline to β -chitin and their antibacterial activity. *J Bioact*
676 *Compat Polym*. 2021;36(1):13-28. doi:10.1177/0883911520973239
- 677 61. Álvarez-Castillo E, Bengoechea C, Felix M, Guerrero A. Freeze-Drying versus Heat-Drying:
678 Effect on Protein-Based Superabsorbent Material. *Processes*. 2021;9(6):1076.
679 doi:10.3390/pr9061076
- 680 62. Zhou G, Liu J, Wang G, et al. Effect of Ultrasonic Treatment on Freeze-thaw Stability of Soy
681 Protein Isolate Gel. *J Oleo Sci*. 2019;68(11):1113-1123. doi:10.5650/jos.ess19167
- 682 63. Yang D, Yuan Y, Wang L, et al. A review on konjac glucomannan gels: microstructure and
683 application. *Int J Mol Sci*. 2017;18(11). doi:10.3390/ijms18112250
- 684 64. Vinatier C, Guicheux J, Daculsi G, Layrolle P, Weiss P. Cartilage and bone tissue engineering
685 using hydrogels. *Biomed Mater Eng*. 2006;16:S107-S113. Accessed January 16, 2024.
686 [https://www.researchgate.net/publication/6962154_Cartilage_and_bone_tissue_engineering_u](https://www.researchgate.net/publication/6962154_Cartilage_and_bone_tissue_engineering_using_hydrogels/figures?lo=1&utm_source=google&utm_medium=organic)
687 [sing_hydrogels/figures?lo=1&utm_source=google&utm_medium=organic](https://www.researchgate.net/publication/6962154_Cartilage_and_bone_tissue_engineering_using_hydrogels/figures?lo=1&utm_source=google&utm_medium=organic)
- 688 65. Piccoli V, Martínez L. Ionic liquid solvation of proteins in native and denatured states. *J Mol*
689 *Liq*. 2022;363:119953. doi:10.1016/j.molliq.2022.119953
- 690 66. Bui-Le L, Clarke CJ, Bröhl A, et al. Revealing the complexity of ionic liquid–protein
691 interactions through a multi-technique investigation. *Commun Chem*. 2020;3(1):55.
692 doi:10.1038/s42004-020-0302-5
- 693 67. Konno K, Young-Je CHO, Yoshioka T, Shinho P, Seki N. Thermal denaturation and autolysis
694 profiles of myofibrillar proteins of mantle muscle of jumbo squid *Dosidicus gigas*. *Fisheries*
695 *Sci*. 2003;69(1):204-209. doi:10.1046/j.1444-2906.2003.00607.x
- 696 68. Paredi ME, Tomas MC, Crupkin M, Añón MC. Thermal Denaturation of Muscle Proteins
697 from Male and Female Squid (*Illex argentinus*) at Different Sexual Maturation Stages. A
698 Differential Scanning Calorimetric Study. *J Agric Food Chem*. 1996;44(12):3812-3816.
699 doi:10.1021/jf960096+
- 700 69. Piccoli V, Martínez L. Correlated counterion effects on the solvation of proteins by ionic
701 liquids. *J Mol Liq*. 2020;320:114347. doi:10.1016/j.molliq.2020.114347

- 702 70. Rieder A, Dhingra S, Khakharia P, et al. Understanding Solvent Degradation: A Study from
703 Three Different Pilot Plants within the OCTAVIUS Project. *Energy Procedia*. 2017;114:1195-
704 1209. doi:10.1016/j.egypro.2017.03.1376
- 705 71. Kasprzak D, Liu J. Chitin and cellulose as constituents of efficient, sustainable, and flexible
706 zinc-ion hybrid supercapacitors. *Sustainable Materials and Technologies*. 2023;38:e00726.
707 doi:10.1016/j.susmat.2023.e00726
- 708 72. Sun J, Shi J, Murthy Konda NVSN, et al. Efficient dehydration and recovery of ionic liquid
709 after lignocellulosic processing using pervaporation. *Biotechnol Biofuels*. 2017;10:154.
710 doi:10.1186/s13068-017-0842-9
- 711 73. Muñoz I, Rodríguez C, Gillet D, M. Moerschbacher B. Life cycle assessment of chitosan
712 production in India and Europe. *Int J Life Cycle Assess*. 2017;23(5):1-10. doi:10.1007/s11367-
713 017-1290-2
- 714 74. Maeda Y, Jayakumar R, Nagahama H, Furuike T, Tamura H. Synthesis, characterization and
715 bioactivity studies of novel beta-chitin scaffolds for tissue-engineering applications. *Int J Biol*
716 *Macromol*. 2008;42(5):463-467. doi:10.1016/j.ijbiomac.2008.03.002
- 717 75. Barikani M, Oliaei E, Seddiqi H, Honarkar H. Preparation and application of chitin and its
718 derivatives: a review. *Iran Polym J*. 2014;23(4):307-326. doi:10.1007/s13726-014-0225-z
- 719 76. Gomes JM, Silva SS, Reis RL. Exploring the Use of Choline Acetate on the Sustainable
720 Development of α -Chitin-Based Sponges. *ACS Sustain Chem Eng*. 2020;8(35):13507-13516.
721 doi:10.1021/acssuschemeng.0c05076
- 722 77. Nie J, Mou W, Ding J, Chen Y. Bio-based epoxidized natural rubber/chitin nanocrystals
723 composites: Self-healing and enhanced mechanical properties. *Composites Part B:*
724 *Engineering*. 2019;172:152-160. doi:10.1016/j.compositesb.2019.04.035
- 725 78. Liang K, Zhou Y, Ji Y. Full biodegradable elastomeric nanocomposites fabricated by chitin
726 nanocrystal and poly(caprolactone-diol citrate) elastomer. *J Bioact Compat Polym*.
727 2019;34(6):453-463. doi:10.1177/0883911519881728
- 728 79. Martinez CLM, Ocaño-Higuera V, Jiménez GMS, Marquez Rios E, Suarez-Jimenez G. Squid
729 protein characteristics and their potential industrial applications. *Interciencia*. 2016;41(8):520-
730 525.
- 731 80. Wilfinger D, Kuehn A, Takacs S, Galli-Novak E, Machan B, Aberer W. Occupational allergic
732 contact urticaria to tropomyosin from squid. *Allergol Select*. 2020;4:129-134.
733 doi:10.5414/ALX02121E